Chinese J. Chem. Eng., 11 (5) 583 – 588 (2003)

Estimation of Separation of Electrolytes and Organic Compounds by Nanofiltration Membranes Using an Irreversible Thermodynamic Model

Pallab Ghosh*
Reverse Osmosis Division, Central Salt and Marine Chemicals Research Institute, Bhavnagar 364002, Gujarat, India

Abstract Nanofiltration separation has become a popular technique for removing large organic molecules and inorganic substances from water. It is achieved by a combination of three mechanisms: electrostatic repulsion, sieving and diffusion. In the present work, a model based on irreversible thermodynamics is extended and used to estimate rejection of inorganic salts and organic substances. Binary systems are modeled, where the feed contains an ion that is much less permeable to the membrane as compared with the other ion. The two model parameters are estimated by fitting the model to the experimental data. Variation of these parameters with the composition of the feed is described by an empirical correlation. This work attempts to describe transport through the nanofiltration membranes by a simple model.

Keywords diffusion, Donnan equilibrium, electrostatic repulsion, ion adsorption, irreversible thermodynamics, nanofiltration, polymeric membranes, steric hindrance, surface charge

1 INTRODUCTION

Nanofiltration membranes developed over the last decade have been used widely in a large number of applications. Some important uses are: removal of salts and organic compounds from drinking water, removal of heavy metal ions and colored substances from industrial wastewater, separation of salt from cheese whey and desulfatation of seawater for offshore oil-well applications. A major characteristic of the nanofiltration membranes is the presence of charge on the surface of their pores. Most commercial nanofiltration membranes are negatively charged. Their rejection layer (*i.e.* the dense polymeric layer that comes into contact with the feed solution) is usually made of sulfonated polysulfone, polyvinyl alcohol or cellulose acetate[1]. The pore size distribution of nanofiltration membranes falls between 0.5—2 nm[2], which is higher than that of highly dense reverse osmosis membranes, but lower than that of ultrafiltration membranes. The mechanism of transport of solute and solvent through the nanofiltration membranes has been suggested to be controlled by diffusivities of the permeating species, their charge and size. Thus, Na_2SO_4 is more rejected by a negatively charged nanofiltration membrane as compared with NaCl, because of higher valency, lower diffusivity and larger size of SO_4^{-2} ion. For large neutral organic molecules having molecular weight greater than approximately 300, the exclusion is mainly based on steric effects. Two models have been extensively used for modeling transport through the nanofiltration membranes: (1) the extended Nernst-Planck equation and (2) the Spiegler-Kedem model. According to the extended Nernst-Planck (ENP) model, the ion flux through the membrane pores is decided by three factors: (1) convection (2) diffusion and (3) migration in the electric field generated by streaming of ions during the flow[3–5]. This is the most detailed bulk-transport model that attempts to represent the actual process, taking into account the Donnan partitioning, steric hindrance and surface charge of the membrane. However, this model requires information on the hindrance parameters for convection and diffusion, which is not readily available.

The Spiegler-Kedem model is based upon irreversible thermodynamics. Several workers have used this model in reverse osmosis and nanofiltration applications[6–11]. In this approach, the membrane is considered as a "black-box". The nature of the membrane (*i.e.* its charge and density) does not affect the transport activities of ions and solvent through it. This model is useful for quick estimation of rejection performance of the membrane. In the present communication, the irreversible thermodynamics model proposed by Spiegler and Kedem is used to analyze the flux-rejection data reported for several commercial nanofiltration membranes. A modification is incorporated to account for the semi-permeability in a binary feed. Selectivity in separation of monovalent and divalent ions is modeled. Variation of the two model parameters with system properties is studied. This work is aimed to investigate the suitability of this model to describe transport through the nanofiltration membranes.

2 MODEL

According to the thermodynamics of irreversible

Received 2002-12-09, accepted 2003-09-06.
* Present address: Department of Chemical Engineering, Indian Institute of Technology Guwahati, Guwahati 781039, India. E-mail: pallabg@iitg.ernet.in

process, flow of each component in a solution is related to the flows of other components. The model states that the fluxes of solute and solvent are directly related to the chemical potential differences between the two sides of the membrane. Either concentration or pressure gradient causes the chemical potential gradient. The solvent transport is due to the pressure gradient across the membrane and the solute transport is due to concentration gradient and convective coupling to the volume flow. The membrane is represented by a series of thin slices of solid material that are separated by thin layers of salt solution, which are in equilibrium with the adjacent membrane layers. The transport equations proposed by Spiegler and Kedem[6] are given by

$$J_V = -\overline{L}_p \left(\frac{dp}{dx} - \sigma \frac{d\pi}{dx} \right) \tag{1}$$

and

$$N_s = -\overline{P}_s \frac{dc}{dx} + (1-\sigma) c J_V \tag{2}$$

where N_s and J_v are solute and solvent fluxes, respectively. σ is a coupling coefficient, known as "reflection coefficient". $\overline{L}_p$ is the specific hydraulic permeability, $\overline{P}_s$ is the local solute permeability and c is salt concentration in virtual solutions adjacent to the membrane layers. The overall solute permeability is defined as

$$P_s = \frac{\overline{P}_s}{\delta} \tag{3}$$

Integrating Eq. (2) over the entire membrane thickness (δ) and using the relationships $c_s^P = N_s/J_V$ and $R = 1 - c_s^P/c_s^F$, the expression for rejection is obtained as

$$R = 1 - \frac{(1-\sigma)}{1 - \sigma \exp\left\{ -\dfrac{(1-\sigma)J_V}{P_s} \right\}} \tag{4}$$

The imperfection of the membrane is characterized by the reflection coefficient, σ. When an osmotic difference ($\Delta\pi$) across an imperfectly semipermeable membrane is compensated by an applied pressure (Δp) so that the volumetric flow is zero, Δp is found to be smaller than $\Delta\pi$. The ratio between these two is defined as σ, *i.e.*

$$\sigma = \left(\frac{\Delta p}{\Delta \pi} \right)_{J_V = 0} \tag{5}$$

In an ideally semipermeable membrane, $\sigma = 1$. In an entirely unselective membrane in which a concentration gradient does not cause volumetric flow at all, $\sigma = 0$. Thus, σ is a measure of the degree of semipermeability of the membrane reflecting its ability to pass solvent in preference to solute.

The parameters, σ and P_s, are assumed to be constants across a membrane. This has been supported experimentally for uncharged membranes. The friction theory of transport makes this assumption plausible. However for charged nanofiltration membranes, P_s and σ can be functions of solute concentration. Correlation of the form: $P_s = \alpha(c^F)^\nu$, has been proposed to account for the variation of P_s with concentration of solute[8]. The Spiegler-Kedem model does not account for the charge on the membrane. Attempts have been made to incorporate the charge effect[12,13].

Equation (4) can be modified to include the Donnan effect when a membrane-impermeable ion is present in the feed solution[7-9]. It is assumed that the salt concentration after a first slice of membrane is in Donnan Equilibrium with the feed solution. The expression for rejection of membrane-permeable salt is given by

$$R_s = 1 - \frac{(1-\sigma)\beta}{1 - \sigma F} \tag{6}$$

where

$$\beta = [1 + z c_I^F / c_-^F]^{1/2} \tag{7}$$

and

$$F = \exp\left\{ -\frac{(1-\sigma)J_V}{P_s} \right\} \tag{8}$$

Where "z" is the valency of the membrane-impermeable ion. The Spiegler-Kedem model is useful in this form to predict rejection when a membrane-impermeable ion is present in a binary feed solution.

However, when the feed solution contains a mixture of NaCl and Na_2SO_4, SO_4^{-2} may not be completely impermeable to the nanofiltration membrane, although $R_{SO_4^{-2}} > R_{Cl^-}$. The system is schematically depicted in Fig. 1. In this case, Eq. (6) can be modified by taking into account the rejection of the semi-impermeable ion. The integrated form of Eq. (2) is the starting point, which can be written as

$$F = \frac{(1-\sigma)J_V c_s^F - N_s}{(1-\sigma)J_V c_s^P - N_s} \tag{9}$$

Let us consider a system in which the feed solution contains a univalent common cation, a univalent membrane permeable anion and a polyvalent anion (of valency z) that is semi-permeable through the membrane (see Fig. 1). The rejection of the semi-permeable anion is considerably higher than that of the membrane permeable anion. The electroneutrality condition in the feed and permeate solution leads to the following equations

$$c_+^F = c_-^F + z c_I^F \tag{10}$$

$$c_+^P = c_-^P + z c_I^P \tag{11}$$

Mean thermodynamic activity of salt having high permeability is given by

$$a_s^F = (a_+^F \cdot a_-^F)^{1/2} \tag{12}$$

and

$$a_s^P = (a_+^P \cdot a_-^P)^{1/2} \quad (13)$$

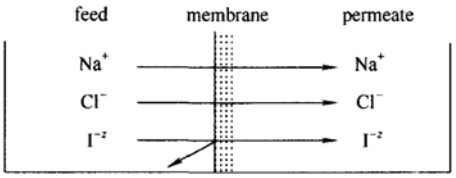

Figure 1 Schematic representation of the binary feed system
(the polyvalent anion is not totally rejected by the membrane)

The difference in activity across the membrane is assumed to be the sole driving force governing the flux of the membrane permeable salt. For simplicity, unit activity coefficients are assumed.

$$c_s^F = (c_+^F \cdot c_-^F)^{1/2} = [(c_-^F + z c_I^F) c_-^F]^{1/2} \quad (14)$$

$$c_s^P = (c_+^P \cdot c_-^P)^{1/2} = [(c_-^P + z c_I^P) c_-^P]^{1/2} \quad (15)$$

and

$$N_s = c_-^P \cdot J_v \quad (16)$$

The rejections of membrane permeable salt (R_s) and semi-permeable salt (R_I) are defined as follows

$$R_s = 1 - c_-^P / c_-^F \quad (17)$$

and

$$R_I = 1 - c_I^P / c_-^F \quad (18)$$

Eq. (9) then becomes,

$$F = \frac{(1-\sigma)\beta - (1-R_s)}{(1-\sigma)\left\{(1-R_s)^2 + z(1-R_I)(1-R_s)\frac{c_I^F}{c_-^F}\right\}^{1/2} - (1-R_s)} \quad (19)$$

Eq. (19) can be solved to obtain R_s, the rejection of the membrane permeable salt in presence of highly rejected membrane semi-permeable salt. The additional information required in this case as compared with Eq. (6) is the rejection of the semi-permeable ion (R_I).

In the special case of total rejection of the ion I^{-z}, *i.e.* $R_I = 1$, Eq. (19) reduces to Eq. (6). For a single solute system, Eq. (4) can be used to predict rejection, whereas, for a feed solution containing a common cation and one semi-permeable anion, Eq. (19) may be used.

3 RESULTS AND DISCUSSION

Equations (4) and (19) predict the variation of rejection of solute with volume flux. Eq. (19) is solved by the Newton-Raphson method. σ and P_s are obtained by minimizing the sum of squares of errors between the model prediction and the experimental data. A constraint is put on σ so that its value can not exceed unity. The fits of the model (indicated by solid lines) to the experimental flux-rejection data taken from the literature for several nanofiltration membranes are shown in Figs. 2—7. In all the cases, solute rejection increases with flux. This is due to the preferential passage of water through the membrane, which increases with increase in flux. The two model parameters, σ (reflection coefficient) and P_s (solute permeability) are shown in each figure. The variation of P_s with salt concentration is depicted in Fig. 8.

3.1 Rejection in single solute systems

Results from three single solute systems are shown in Figs. 2—4. An increase in the rejection of NaCl with solvent flux is shown in Fig. 2. In this case, rejection decreases with increase in concentration of NaCl. The reflection coefficient remains constant in all the cases, and the solute permeability increases with the solute concentration. Similar results are observed with feed containing Na_2SO_4, shown in Fig. 3. The trends in this case are similar to those for NaCl (Fig. 2). The solute permeability (P_s) increases with concentration. In both these systems, Eq. (4) fits to the experimental data well. Decrease in salt rejection with increase in concentration of salt is a manifestation of presence of charge on the pores of these membranes. Both of these nanofiltration membranes have negatively charged rejection layers. The charge on the membrane surface depends on the valencies of the cations and anions, and the concentration of these ions in the feed solution[15]. Some results based on electrokinetic measurements reveal interesting information. For a poyethersulfone membrane in contact with Na_2SO_4 solution, it has been found that with increase in concentration of Na_2SO_4, some Na^+ ions adsorb on the membrane surface, thereby reducing the electrostatic repulsion exerted by the membrane[16].

At sufficiently high concentrations of Na_2SO_4, adsorption of counterion overcompensates the adsorption of sulfate ions, and the inherently negative charged membrane acquires positive charge. This enhances passage of salt through the membrane, thus reducing rejection. Moreover, increase in salt concentration reduces Donnan partitioning, which reduces rejection.

However, in water-$CaCl_2$ system (Fig. 4) with negatively charged Desal-5DK membrane, the effect of concentration is exactly the reverse of those shown in Figs. 2 and 3. The electrokinetic measurements did not indicate build-up of Cl^- ions on the membrane surface that could have increased repulsion of ions by the membrane leading to a higher rejection. It has been suggested that the dielectric constant of the solution in the pores of the membrane decreases with an increase in the concentration of $CaCl_2$, which leads to higher exclusion of $CaCl_2$ from the membrane[15]. In this system, P_s decreases with solute concentration,

which is opposite to that observed in Figs. 2 and 3. The reflection coefficient (σ) is found to increase with the solute concentration in the feed.

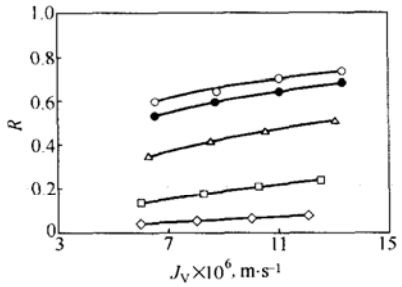

Figure 2 Variation of rejection of NaCl as a function of volume flux and concentration in the feed in a single solute system

(The experimental data are taken from Ref. [13], NTR-7450 nanofiltration membrane of Nitto-Denko that has negatively charged sulfonated polyethersulfone rejection layer was used)

c^F, mol·m^{-3}: ○ 2; ● 10; △ 30; □ 100; ◇ 500

$P_s \times 10^6$, m·s^{-1}: ○ 3.5; ● 4.8; △ 10.3; □ 34.0; ◇ 125.0

$\sigma = 0.9$; solid lines indicate the fit of Eq. (4)

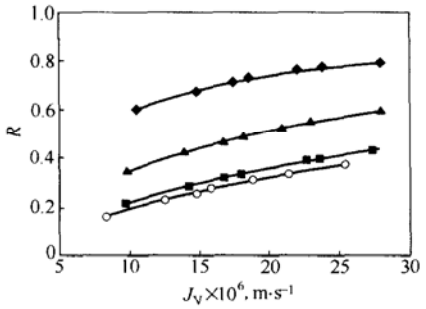

Figure 3 Variation of rejection of Na_2SO_4 with volume flux and concentration in the feed in a single solute system

(The experimental data are taken from Ref. [14]. CA-30 nanofiltration membrane of Hoechst that has negatively charged cellulose acetate rejection layer was used)

c^F, mol·m^{-3}: ◆ 5.0; ▲ 12.5; ■ 25.0; ○ 100.0

$P_s \times 10^6$, m·s^{-1}: ◆ 6.5; ▲ 18.0; ■ 34.0; ○ 40.0

$\sigma = 0.96$; solid lines indicate the fit of Eq. (4)

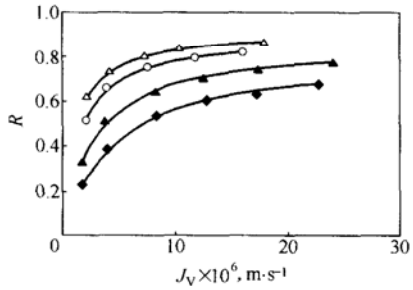

Figure 4 Variation of rejection of $CaCl_2$ with volume flux and concentration in the feed in a single solute system

(The experimental data are taken from Ref. [15]. Dasal-5DK nanofiltration membrane of Desalination Systems that has negatively charged polyamide rejection layer was used)

c^F, mol·m^{-3}: △ 50; ○ 10.0; ▲ 2.0; ◆ 0.5

σ: △ 0.88; ○ 0.85; ▲ 0.80; ◆ 0.73

$P_s \times 10^6$, m·s^{-1}: △ 1.1; ○ 1.5; ▲ 2.7; ◆ 4.2

solid lines indicate the fit of Eq. (4)

3.2 Rejection of large organic molecules

Rejection of three polysaccharides is shown in Fig. 5. With increase in molecular weight and size, rejection increases. P_s decreases whereas, σ increases with solute size. The Steric-Hindrance-Pore (SHP) theory[12] is used to explain the relationship between these two model parameters and the structural properties of the membrane. According to this theory, the solute molecule encounters steric hindrance inside the pore and interacts with the pore walls. The variations of P_s and σ with solute size are given by the following relations[12]

$$P_s = (1-\eta)^2 D_s \left(\frac{A_K}{\delta}\right) \tag{20}$$

$$\sigma = 1 - (1-\eta)^2 \left(1 + \frac{16}{9}\eta^2\right)[2 - (1-\eta)^2] \tag{21}$$

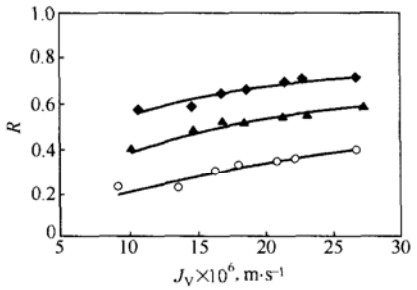

Figure 5 Rejection of large organic molecules of different molecular weight and size, as function of volume flux in a single solute system

[The experimental data are taken from Ref. [14]. CA-30 nanofiltration membrane of Hoechst (MWCO=1000 u) was used]

◆ Raffinose: $\sigma = 0.80$, $P_s = 5.7 \times 10^{-6}$ m·s^{-1};

▲ Maltose: $\sigma = 0.75$, $P_s = 10.9 \times 10^{-6}$ m·s^{-1};

○ Galactose: $\sigma = 0.70$, $P_s = 25.0 \times 10^{-6}$ m·s^{-1};

solid lines indicate the fit according to Eq. (14)

where η is the ratio of the radii of solute and membrane pore. D_s is the diffusivity of solute and (A_K/δ) is the ratio of membrane porosity to the thickness of membrane rejection layer. Eq. (20) predicts a decrease in solute permeability with an increase in its size, which is found to be true. The structural parameter (A_K/δ) can be estimated using the fitted values of P_s. It is estimated that $A_K/\delta = 1.45 \times 10^5$ m^{-1} corresponding to pore radius, $r_P = 0.8$ nm. These values agree well with those estimated using the extended Nernst-Planck Equation for uncharged solutes[14]. The value obtained from the extended Nernst-Planck Equation is, $r_P = 0.94$ nm for the same (A_K/δ). Eq. (21) predicts that σ should increase with the ratio of solute radius to pore radius (η). From galactose to raffinose, the Stokes radius of solute increases from 0.37 nm to 0.58 nm. However, the increase in σ predicted by Eq. (20) is steeper than that

obtained by fitting the experimental data. The possible reason for this variation can be the tortuous and interconnected nature of the pores present in this CA-membrane that is not taken into account by the SHP model.

3.3 Rejection of NaCl in a binary feed solution of NaCl and Na_2SO_4

Negatively charged nanofiltration membranes repel divalent anions more strongly than monovalent anions. This repulsion increases with increase in charge density on the surface of the membrane. Thus, the sulfate ions are more strongly repelled than the chloride ions. Moreover, the Stokes radius of the sulfate ion is double to that of the chloride ion and the diffusivity is nearly half. All these factors cause a much higher rejection of Na_2SO_4 as compared with NaCl. Conventional thin-film-composite (TFC) reverse osmosis membranes (*e.g.* FT-30) reject both of these almost totally, showing little selectivity. These membranes have negligible surface charge. That is why these membranes are not suitable for selective separation of ions. Since the sulfate ion behaves like a semi-permeable anion with high rejection, Eq. (19) can be used to estimate the rejection of NaCl, which has higher permeability. An interesting observation in these two-component systems is, as the concentration of sulfate is increased in the feed keeping total concentration fixed, the rejection of NaCl becomes negative. Negative rejection implies that the concentration of NaCl is higher in the permeate than in the feed. This happens because of the Donnan equilibrium, discussed in Section 2. Eq. (19) can predict this negative rejection, which is observed in the low flux region. In Fig. 6, results are shown for NTR-7450 membrane. When the concentration of Na_2SO_4 is four times that of NaCl, the rejection remains negative throughout the flux-range studied. On the other hand, when the molefraction of sulfate is 0.2, the rejection of NaCl is always positive. σ remains independent of the concentration of NaCl. The results shown in Fig. 7 also demonstrate similar facts. Here the total solute concentration in the feed is smaller than that in the system shown in Fig. 6. Negative rejection is observed when sulfate concentration in the feed is high. It is usually observable at the low-flux region. A comparison of Fig. 6 and Fig. 7 reflects the effect of total solute concentration. At higher total solute concentration in the feed, the negative rejection is more pronounced.

In all these systems, the model proposed by Eq. (19) fits the flux-rejection data well. The solute permeability shows a definite trend, *i.e.* it increases with the concentration of more permeable solute.

3.4 Dependence of solute permeability with solute concentration

It has been suggested in the Ref. [8] that P_s varies with c^F obeying the relation: $P_s = \alpha(c^F)^\nu$, where α and ν are constants. The results obtained in this study indicate that the constant α is always positive. Usually, its value is much less than unity. The parameter ν is positive in all systems studied, except in the system of water-$CaCl_2$. The variation of P_s with c^F is depicted in Fig. 8. The values of α and ν are presented in Table 1.

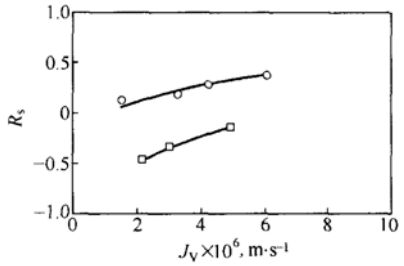

Figure 6 Rejection of NaCl from a binary feed solution of NaCl and Na_2SO_4 as function of volume flux

[The figure depicts shift in rejection from negative to positive with increase in concentration of NaCl keeping the total concentration of salt in the feed constant at 50 mol·m^{-3}. Data are taken from Ref. [13] where NTR-7450 nanofiltration membrane of Nitto-Denko was used. The rejection data of SO_4^{-2} taken from the same source are used in Eq. (19)]
○ chloride:sulfate=4.00, $\sigma = 0.7$, $P_s = 3.7 \times 10^{-6}$ m·s^{-1};
□ chloride:sulfate=0.25, $\sigma = 0.7$, $P_s = 1.5 \times 10^{-6}$ m·s^{-1}; solid lines indicate model fit according to Eq. (19)

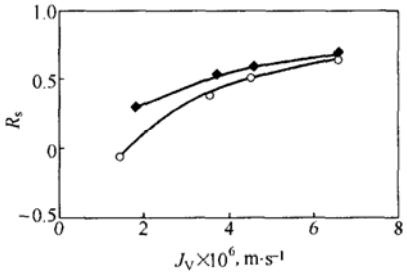

Figure 7 Rejection of NaCl from a binary feed solution of NaCl and Na_2SO_4 as function of volume flux

[The figure depicts shift in rejection from negative to positive with increase in concentration of NaCl keeping the total concentration in the feed constant at 10 mol·m^{-3}. Data are taken from Ref. [13] where NTR-7450 nanofiltration membrane of Nitto-Denko was used. The rejection data of SO_4^{-2} taken from the same source are used in Eq. (19)]
◆ chloride:sulfate=4.00, $\sigma = 0.97$, $P_s = 2.3 \times 10^{-6}$ m·s^{-1};
○ chloride:sulfate=0.25, $\sigma = 0.97$, $P_s = 0.8 \times 10^{-6}$ m·s^{-1}; solid lines indicate the fit of Eq. (19)

Table 1 Parameters α and ν in the empirical relationship [$P_s = \alpha(c^F)^\nu$ for three systems]

System	$\alpha \times 10^6$, m·s^{-1}	ν
water-NaCl (Fig. 2)	1.4	0.68
water-Na_2SO_4 (Fig. 3)	3.4	0.59
water-$CaCl_2$ (Fig. 4)	3.3	−0.30

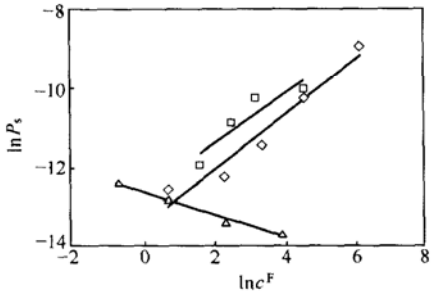

Figure 8 Variation of solute permeability with concentration of solute in the feed
□ system of Na_2SO_4-water; ◇ system of NaCl-water; △ system of $CaCl_2$-water

4 CONCLUSIONS

The present work demonstrates the suitability of the Spiegler-Kedem model for estimation of rejection in nanofiltration applications. This will be important to describe separation in two-component systems having ions of different valency, utilizing the principles of Donnan equilibrium.

This effect may be utilized in some applications such as, removal of salt from salty cheese whey, desulfatation of seawater, and removal of dyestuff from pulp wastewater. The small variation of reflection coefficient with solute concentration makes it easier to deal with only one adjustable concentration dependent parameter, *i.e.* solute permeability (P_s). Variation of P_s with solute concentration is shown to follow a definite exponential relationship. However, it is found that for certain systems, the sign of the coefficient, ν, can be negative, although for most systems both of these coefficients are positive. The variation of reflection coefficient (σ) with the size of organic molecule is found to obey the pattern predicted by the steric hindrance model. It should be possible to correlate P_s with the zeta potential on the membrane surface, which varies with feed concentration.

NOMENCLATURE

A_K	membrane porosity
a	activity, $mol \cdot m^{-3}$
c	concentration, $mol \cdot m^{-3}$
D_s	diffusivity of solute, $m^2 \cdot s^{-1}$
F	variable, defined by Eq. (8)
J_V	volume flux, $m \cdot s^{-1}$
$\overline{L}_p$	specific hydraulic permeability, $m^4 \cdot N \cdot s^{-1}$
N	molar flux, $mol \cdot m^{-2} \cdot s^{-1}$
P_s	overall solute permeability, $m \cdot s^{-1}$
$\overline{P}_s$	local solute permeability, $m^2 \cdot s^{-1}$
p	pressure, Pa
R	rejection
r_P	pore radius, m
x	direction of flow, m
z	valency
α	constant, $m \cdot s^{-1}$
β	variable, defined by Eq. (7)
δ	thickness of the rejection layer, m
η	ratio of solute radius to pore radius
ν	constant
π	osmotic pressure, Pa
σ	reflection coefficient

Superscripts

F	feed
P	permeate

Subscripts

I	impermeable or semi-permeable ion
s	solute
+	cation
−	anion

REFERENCES

1 Raman, L.P., Cheryan, M., Rajagopalan, N., "Consider nanofiltration for membrane separations", *Chem. Eng. Prog.*, **90** (3), 68 (1994).
2 Bowen, W.R., Mohammad, A.W., Hilal, N., "Characterisation of nanofiltration membranes for predictive purposes—Use of salts, uncharged solutes and atomic force microscopy", *J. Membr. Sci.*, **126** (1), 91 (1997).
3 Tsuru, T., Nakao, S., Kimura, S., "Calculation of ion rejection by extended Nernst-Planck equation with charged reverse osmosis membranes for single and mixed electrolyte solutions", *J. Chem. Eng. Japan*, **24** (4), 511 (1991).
4 Dresner, L., "Some remarks on the integration of the extended Nernst-Planck equations in the hyperfiltration of multicomponent solutions", *Desalination*, **10** (1), 27 (1972).
5 Bowen, W.R., Mohammad, A.W., "Diafiltration by nanofiltration: Prediction and optimization", *AIChE J.*, **44** (8), 1799 (1998).
6 Spiegler, K.S., Kedem, O., "Thermodynamics of hyperfiltration (reverse osmosis): Criteria for efficient membranes", *Desalination*, **1** (4), 311 (1966).
7 Perry, M., Linder, C., "Intermediate reverse osmosis ultrafiltration (RO/UF) membranes for concentration and desalting of low molecular weight organic solutes", *Desalination*, **71** (3), 233 (1989).
8 Schirg, P., Widmer, F., "Characterisation of nanofiltration membranes for the separation of aqueous dye-salt solutions", *Desalination*, **89** (1), 89 (1992).
9 Gilron, J., Gara, N., Kedem, O., "Experimental analysis of negative salt rejection in nanofiltration membranes", *J. Membr. Sci.*, **185** (2), 223 (2001).
10 Levenstein, R., Hasson, D., Semiat, R., "Utilization of the Donnan effect for improving electrolyte separation with nanofiltration membranes", *J. Membr. Sci.*, **116** (1), 77 (1996).
11 Jitsuhara, I., Kimura, S., "Rejection of inorganic salts by charged ultrafiltration membranes made of sulfonated polysulfone", *J. Chem. Eng. Japan*, **16** (5), 394 (1983).
12 Wang, X.L., Tsuru, T., Togoh, M., Nakao, S., Kimura, S., "Evaluation of pore structure and electrical properties of nanofiltration membranes", *J. Chem. Eng. Japan*, **28** (2), 186 (1995).
13 Tsuru, T., Urairi, M., Nakao, S., Kimura, S., "Reverse osmosis of single and mixed electrolytes with charged membranes: Experiment and analysis", *J. Chem. Eng. Japan*, **24** (4), 518 (1991).
14 Schaep, J., Vandecasteele, C., Mohammad, A.W., Bowen, W.R., "Analysis of the salt retention of nanofiltration membranes using the Donnan-steric partitioning pore model", *Sep. Sci. Technol.*, **34** (15), 3009 (1999).
15 Hagmeyer, G., Gimbel, R., "Modelling the salt rejection of nanofiltration membranes for ternary ion mixtures and for single salts at different pH values", *Desalination*, **117** (1-3), 247 (1998).
16 Ernst, M., Bismarck, A., Springer, J., Jekel, M., "Zeta potential and rejection rates of a polyethersulfone nanofiltration membrane in single salt solutions", *J. Membr. Sci.*, **165** (2), 251 (2000).